Desalination and Water Treatment
www.deswater.com

doi: 10.5004/dwt.2019.24057

155 (2019) 296–310
July

Adsorption mechanism of borate with different calcined layered double hydroxides in a molar ratio of 3:1

Shuang Xu, Jiawen Zhao, Lidan Deng, Jinhua Niu, Xu Zhou, Shuwang Zhang, Xinhong Qiu*, Jinyi Chen*

School of Chemistry and Environmental Engineering, Wuhan Institute of Technology, Wuhan 430073, China, emails: qxinhong@gmail.com (X. Qiu), jychwit@163.com (J. Chen)

Received 4 September 2018; Accepted 1 March 2019

ABSTRACT

Layered double hydroxides (LDHs) with a molar ratio of 3:1, which contain different divalent metals (Zn-LDH, Mg-LDH, and Ca-LDH), were synthesized. They were calcined at 500°C (Zn-CLDH, Mg-CLDH, and Ca-CLDH) for borate removal. The characterization of different CLDHs before and after adsorption of boric acid was performed by XRD, FTIR, and SEM. For Ca-CLDH (3:1), the main removal mechanism was the formation of ettringite with borate, which is the same as Ca-CLDH (2:1). However, the latter has a much higher adsorption of borate than the former, because for Ca-CLDH (2:1), the amount of ettringite produced during regeneration is more than that of Ca-CLDH (3:1). For Zn-CLDHs (3:1 and 2:1), borate was removed completely by ion exchange and intercalation. However, the adsorption rate of Zn-CLDH (2:1) is higher than that of Zn-CLDH (3:1), even though the final adsorption capacity is similar. In addition, Zn-LDH (2:1) containing polymerized boron formed in a short time, but as the reaction progresses, more Zn-LDH (3:1) containing polymerized boron is gradually formed. For two ratios of Mg-CLDHs, borate was first immobilized on the surface of metal oxide by electrostatic adsorption and then entered the interlayer of Mg-LDHs by intercalation, resulting in a decrease in borate concentration. However, Mg-LDH (3:1) has a faster and better adsorption of borate than Mg-LDH (2:1), and the structure regeneration time of Mg-CLDH (3:1) was shorter than that of Mg-CLDH (2:1). Therefore, when using CLDHs for boron removal, the metal type and ratio of LDHs should be considered.

Keywords: Boron; LDH; Intercalation; Mechanism; Molar ratio

1. Introduction

As one of the essential micronutrients, boron is important for plants, animals, and humans [1–3]. However, in recent years, boric acid has been widely used as an important raw material in various industries, releasing a large amount of boron compound into the environment [4]. In addition, the removal of borate in seawater for production of drinking water is difficult and expensive because of its excellent water solubility [5,6]. Therefore, it is essential to develop an effective method for borate removal [7].

Different methods have been developed for the removal of borate from a solution, such as ion-exchange, coagulation and electrocoagulation, reverse osmosis, and sorption method [8–12]. Some new materials and technologies have also been extensively studied for environmental remediation [13–16]. Among these methods, the adsorption method is useful and advantageous than other methods because it produces less waste during processing and also involves lower costs [17]. At present, layered double hydroxides (LDHs), especially its calcinated products (CLDHs) are considered as one of the effective sorbents for borate removal. The mechanism of borate immobilized by calcinated LDHs has been summarized

* Corresponding authors.

by Theiss et al. [18]; structural regeneration and capture of anions are the primary mechanisms for the high-efficiency absorption of borate in CLDHs. In 2014, Isaacs-Paez et al. [19] reported that the borate removal by CLDHs is a more complex process, and other reactions might occur between CLDHs and borate during the structure regeneration. Based on the sorption mechanisms reported by Demetriou et al. [20] and Sasaki et al. [21], the reactions between Zn-Al-CLDH, Mg-Al-CLDH, and Ca-Al-CLDH with borate are actually a complex process that involves the interactions among CLDHs, newly generated LDHs, borate, and OH^- [22]. Among them, the predominant mechanism of borate removal with Zn-Al-CLDH is through anion exchange and intercalation. Mg-Al-CLDH immobilizes borate into $Mg(OH)_2$ first through surface complexation and electrostatic attraction and then attracts borate as the interlayer anionic layer into the new structure of Mg-Al-LDH. However, the main removal mechanism of borate with Ca-Al-CLDH involves the formation of borate-containing ettringite from the dissolved ions of Ca-Al-LDH. In previous study, the molar ratio of divalent metal ions to trivalent metal ions is 2:1, but when the molar ratio becomes 3:1, the average metal–oxygen bond lengths, metal–oxygen–metal bond angles, and average interatomic distances are changed. These changes affect the microstructure and stability of LDHs by Yan et al. [23,24]; thus, the structural change in these LDHs may cause some differences in removing borate. Based on the above understanding, the following studies were performed.

In this study, (1) the LDHs (3:1) containing different bivalent metal ions are calcined to adsorb boron; (2) the solids obtained before and after the adsorption are characterized; (3) the detailed mechanism and schematic diagram for the adsorption of borate with different CLDHs are given; (4) the adsorption behavior and mechanism of different CLDHs with molar ratios of 2:1 and 3:1 are compared.

2. Experimental method

2.1. Chemicals

Magnesium nitrate hexahydrate ($Mg(NO_3)_2{\cdot}6H_2O$), calcium nitrate tetrahydrate ($Ca(NO_3)_2{\cdot}4H_2O$), zinc nitrate hexahydrate ($Zn(NO_3)_2{\cdot}6H_2O$), aluminum nitrate nonahydrate ($Al(NO_3)_3{\cdot}9H_2O$), urea (CON_2H_4), boric acid (H_3BO_3), and sodium hydroxide (NaOH) were used in special grade as received from WAKO (Osaka, Japan) without further purification.

2.2. Preparation of LDHs with different divalent metals

The similar method [25] was introduced for preparing LDHs with divalent metals of Zn and Mg [Zn-LDH (3:1) and Mg-LDH (3:1)]. $Al(NO_3)_3{\cdot}9H_2O$ (3.09 g) and M^{2+} salt ($Mg(NO_3)_2.6H_2O$, 6.15 g; $Zn(NO_3)_2{\cdot}6H_2O$, 7.14 g) and urea (4.90 g) were dissolved in a beaker to form a clear solution with a total volume of 50 mL. Then, the solution was transferred into a Teflon vessel, which was placed on an oven at 100°C for 36 h. After that, the slurry was separated by centrifugation at 10,000 rpm for 10 min, and the products were rinsed with deionized water and then dried for overnight. A high alkaline condition (pH > 11.5) was required for the LDHs with Ca as the divalent metal so that Ca-LDH cannot be synthesized using the urea method. Microwave-assisted method was used for preparing Ca-LDH (3:1). A solution containing a certain amount of $Ca(NO_3)_2{\cdot}4H_2O$ (5.67 g) and $Al(NO_3)_3{\cdot}9H_2O$ (3.09 g) in a molar ratio of 3:1 was added to 50 mL of 0.5 mol/L $NaNO_3$ solution; the pH was adjusted to 12 with 2 mol/L NaOH. The resulting slurry was transferred into the Teflon vessel and placed in a Milestone Ethos Plus microwave oven. The temperature was increased to 150°C within 10 min and was kept at that temperature for 3 h and then naturally cooled to room temperature. The cooled slurry was subjected to solid–liquid separation through super-centrifugation at 10,000 rpm for 10 min and washed with ultrapure water (Synergy UV, Millipore, USA) several times. The solid residues were then dried overnight in a vacuum freeze drier. Before sorption experiments, all the LDHs were calcined at 500°C for 3 h, so that Zn-CLDH (3:1), Mg-CLDH (3:1), and Ca-CLDH (3:1) were obtained.

2.3. Sorption experiments

Sorption of borate on different calcined products at 500°C was performed in 2.5 mmol/L H_3BO_3. The pH of H_3BO_3 solutions was adjusted to 7.0 with 1 mol/L NaOH. For sorption experiments, 0.100 g of calcined products was added to 40 mL of borate solution, followed by shaking at 100 rpm and at room temperature using a shaking incubator TB-16R (Takasaki Kagaku, Kawaguchi, Japan). At certain time intervals, the supernatants were filtered (0.20 μm) for the determination of total concentrations of B, Ca, Zn, Mg, and Al by inductively coupled plasma-atomic emission spectrometry (ICP-AES, Optima 8300, Perkin Elmer, Massachusetts, USA).

2.4. Characterization

The crystalline phases of various LDHs were determined using an X-ray diffractometer (Ultima IV, Rigaku, Japan) with Cu *Kα* radiation. The accelerating voltage and applied current were 40 kV and 40 mA, respectively, with a scanning speed of 2 min^{-1} and scanning step of 0.02. Fourier transform infrared (FTIR) spectra were recorded using a FTIR 670 Plus spectrophotometer (JASCO, Tokyo, Japan). The morphologies of products calcined at different temperatures were observed using a VE-9800 scanning electron microscope (Keyence, Osaka, Japan) at 20 kV accelerating voltage.

3. Results and discussion

3.1. Characterization

Fig. 1 shows the XRD results with different LDHs before and after calcinations. As shown in Fig. 1(a), the basal characteristic diffraction peaks of Zn-LDH, Mg-LDH, and Ca-LDH before calcinations indicate a good crystalline layered structure. However, the 003 and 006 peaks of Zn-LDH and Mg-LDH samples disappeared after calcination at 500°C under air for 3h (Fig. 1(b)), indicating that the layered structure is damaged at this temperature. For Zn-CLDH and Mg-CLDH, some broad peaks appeared in the spectrum, which are ZnO and MgO according to previous literature [26]. In the meantime, the 002 and 004 peaks of Ca-LDH also disappeared after calcination. However, some different peaks appeared in the XRD pattern of Ca-CLDH, which are assigned to CaO and $Ca(OH)_2$. Some other broad peaks are assigned to $Ca_3AlO_3(OH)_8$ in an amorphous phase [27].

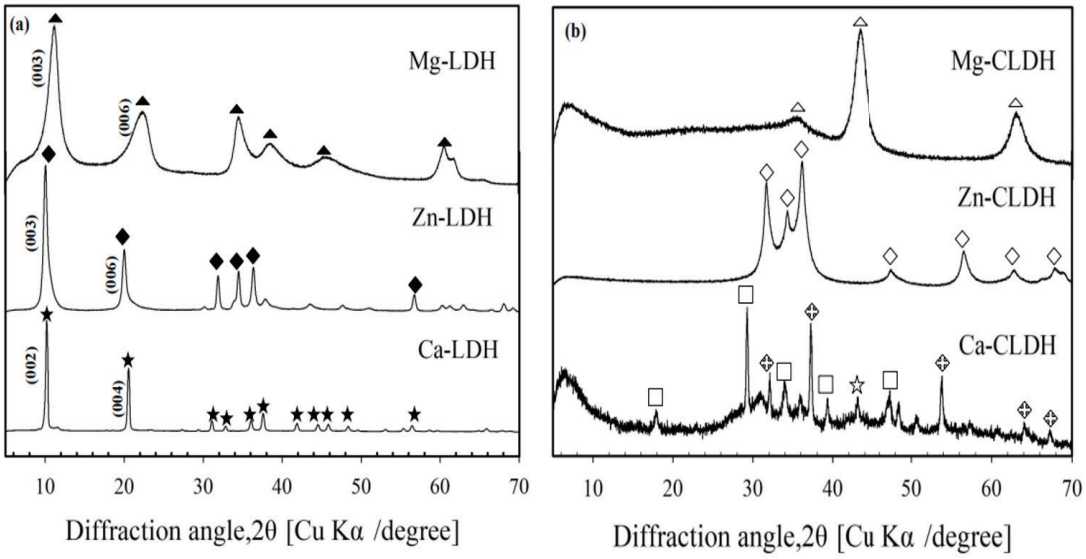

Fig. 1. XRD patterns of Mg-LDH, Zn-LDH, and Ca-LDH (a) before and (b) after calcination at 500°C for 3 h. Symbols: ▲, Mg-LDH; △, Mg-CLDH; ◆, Zn-LDH; ◇, Zn-CLDH; ★, Ca-LDH; □, $Ca(OH)_2$; ✥ CaO; ☆, $Ca_{12}Al_{14}O_{33}$.

3.2. Sorption of borate

Fig. 2 shows that although adsorption results are similar, the average degradation rate of Zn-CLDH (3:1) is faster than Mg-CLDH (3:1). Under the same condition, the ability of Ca-CLDH (3:1) is the worst. In addition, compared with previous literature [22], it was found that the borate concentration is reduced significantly by Zn-CLDH (3:1) within 8 h (Fig. 2), while the borate concentration is reduced by Zn-CLDH (2:1) in only 3 h (Fig. S1) [22]. However, borate is completely removed by Mg-CLDH (3:1) in 8 h, and it takes 48 h for Mg-CLDH (2:1) to achieve the same effect. For Ca-CLDH (3:1), its ability of borate adsorption is much less than that of Ca-CLDH (2:1). The adsorption capacities of different boron adsorbents are shown in Table S1. The adsorption effect of CLDHs is significantly improved and superior to other adsorbents.

The XRD patterns of Zn-CLDH (3:1), Mg-CLDH (3:1), and Ca-CLDH (3:1) before and after the sorption of borate at different times are shown in Fig. 3. As the adsorption time increases, all CLDHs gradually recover their original structure and ultimately regenerated into LDHs after 48 h when the initial boron concentration is 2.5 mmol/L. For Zn-CLDH and Ca-CLDH, their crystal phase was transformed from metallic oxide into LDHs within 40 min, whereas Mg-CLDH needs almost 8 h. Only when the metal oxide dissolves first, the structure of LDHs can be formed by reprecipitation. However, the alkalinity and charge of solid oxides have a certain influence on the dissolution and precipitation rate of metal ions [28]. The higher alkalinity indicates that the metal present in the CLDHs is more likely to lose electrons, to attract OH^- to neutralize the charge and stabilize its structure. Therefore, Figs. 2 and 3 show that Ca-CLDH is transformed rapidly because of a higher basicity. Mg-CLDH has a higher basicity than Zn-CLDH, but its regeneration time is longer than that of Zn-CLDH. This is probably related to their morphology, while Zn-CLDH is spherical and Mg-CLDH is flake.

For Zn-CLDH (3:1), it only takes less than 40 min for most Zn-CLDH to be transformed into Zn-LDH (Fig. 3(a)), which is the same as Zn-CLDH (2:1) (Fig. S2) [22]. In the two XRD patterns, ZnO and Zn-LDH are always present as the reaction progresses. However, there are two types of Zn-LDHs with different interlayer spacings present in the spectrum after 3 h. One of the Zn-LDHs with a smaller value is 7.6 Å, and another is ~10.76 Å. However, with the increase in reaction time, Zn-LDH (3:1) with a larger interlayer spacing gradually increases, and after 48 h, three different crystal phases exist in the pattern. However, Zn-LDH (2:1) with a larger interlayer spacing appears at 3 h, and the peak intensity is very high, but disappears at the next point of time.

For Mg-CLDH (3:1) (Fig. 3(b)), only two types of characteristic peaks are shown in the pattern during the reconstruction, Mg-LDH and MgO. Moreover, the peaks of MgO gradually weaken and finally disappear at 48 h; the phase of Mg-LDH (3:1) appears after 8 h of reaction and gradually becomes the main phase. However, for [22] in Fig. S3, there is almost no change in the peaks of MgO in the first 20 h, and the phase of Mg-LDH (2:1) just appeared after 48 h of reaction. In addition, the concentration of Mg^{2+} and boron species in the solution decreased to a lower level at the same time (Figs. 2 and S1), which is noteworthy.

Unlike the other two types of CLDHs, Ca-CLDH (3:1) is completely transformed into Ca-LDH structure within 40 min (Fig. 3(c)). There are two main diffraction peaks: ettringite [29] and LDH. However, as the reaction time increases, the relative peak intensities of Ca-CLDH (3:1) and ettringite hardly change. However, in Fig. S4, as the phase of Ca-CLDH (2:1) decreases, the ettringite phase gradually increases. With the increase time, $CaCO_3$ also became a major phase [22]. Therefore, the amount of ettringite formed by Ca-CLDH (3:1) regeneration is much smaller than that formed by Ca-LDH (2:1) regeneration.

Fig. 4 shows the FTIR spectra of solid residues before and after the sorption of borate on different CLDHs to determine the mechanisms of borate removal. The IR spectra of

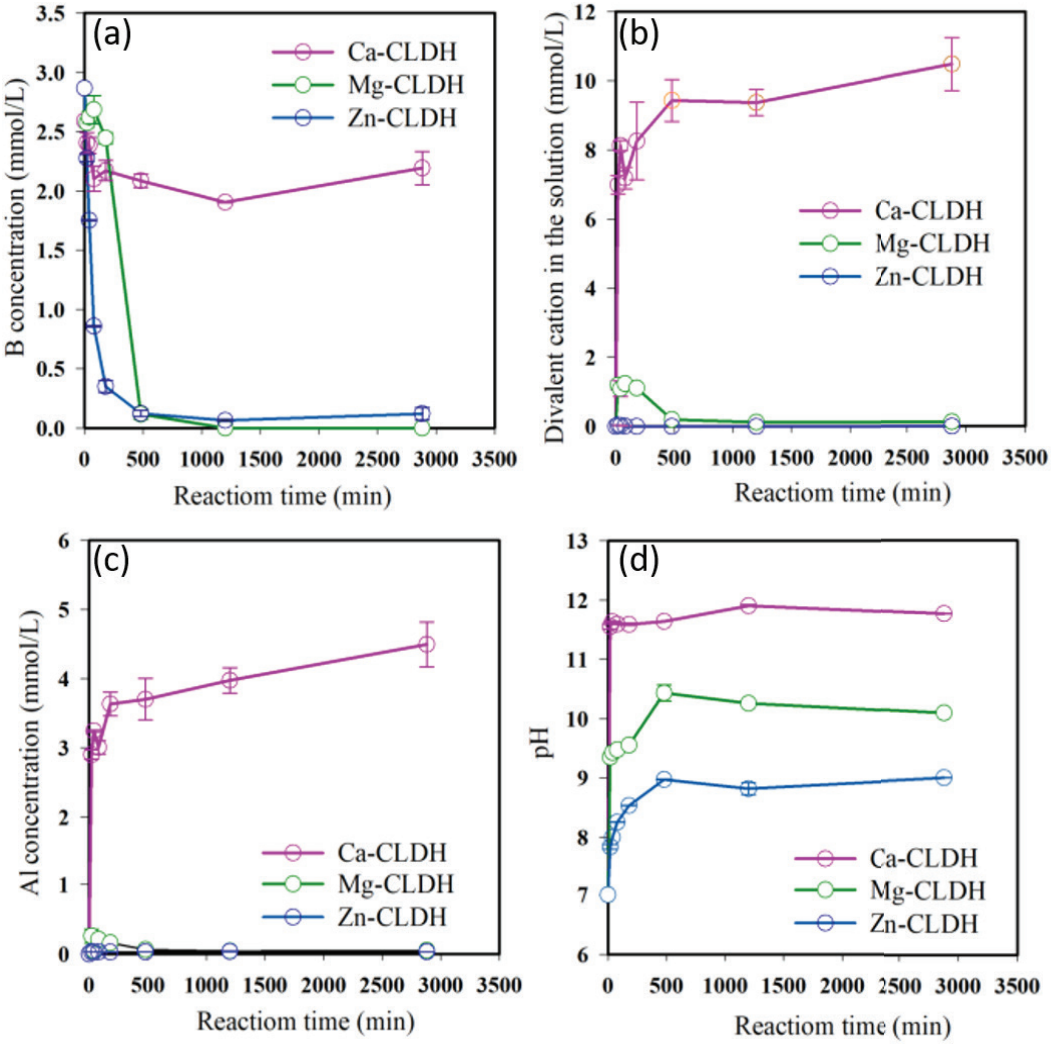

Fig. 2. Changes in (a) B concentrations, (b) divalent cations concentration, (c) Al concentration, and (d) pH during sorption of 2.5 mM B by Mg-CLDH, Zn-CLDH, and Ca-CLDH. Amount of sorbent: 2.5 g/L; initial B concentration: 2.5 mM; initial pH: 7.0.

three types of CLDHs before and after adsorption had some changes, indicating that the adsorption of borate leads to the structural changes.

For Zn-CLDH (Fig. 4(a)) and Mg-CLDH (Fig. 4(b)), broad peaks at ~3,465 cm^{-1} appeared in the samples before and after adsorption, which can be assigned to metal–OH stretching vibrations [30]. The band at ~1636 cm^{-1} can be assigned to the O–H bending vibration of water molecules. The peak at ~1403 cm^{-1} belongs to the O–C vibration absorption peak, because of the interference of CO_2 during the reaction. The peak at ~1,360 cm^{-1} appearing in the adsorbed spectrum of Zn-CLDH and Mg-CLDH can be assigned to CO_3^{2-}, because the regenerated LDHs adsorb CO_2 and H_2O.

Compared with other CLDHs, the FTIR spectrum of Ca-CLDH was different (Fig. 4(c)). For Ca-CLDH and Ca-CLDH-48 h, an absorption peak appears in the region of 3,500–3,700 cm^{-1}, which is caused by the stretching vibration of water molecules and O-H groups in the sample [31]. The characteristic absorption peak of $CaCO_3$ appears at 1,420 cm^{-1}. However, for Ca-CLDH-48h, the corresponding CO_3^{2-} vibration appears at about 1,365 and 856 cm^{-1}, and the peak at 1,365 cm^{-1} overlaps with the peak of $CaCO_3$. In addition, many small peaks appear between 800 and 400 cm^{-1}, which are related to the M–O (or M–O–M) lattice bending vibrations of metal oxides [32].

Fig. 5 shows the SEM pattern of different LDHs and different CLDHs after the adsorption of boron. The morphology of each LDH is not same, and the changes after the calcined products adsorb borate are also different. For Zn-LDH (3:1) (Fig. 5(a)), the morphology is a blossom sphere with flaky debris; after the calcination and sorption of borate (Fig. 5(b)), the spherical structure is tighter, but no significant change was observed in diameter. For the Mg-LDH (3:1) (Fig. 5(c)) and Ca-LDH(3:1) (Fig. 5(e)), before the adsorption, the morphology is a smooth hexagonal sheet-like structure, and some of them are stacked. However, after the adsorption, the basic morphology of Mg-CLDH-48h (Fig. 5(d)) did not change, but its platelets became very rough, while the morphology of Ca-CLDH-48h (Fig. 5(f)) changed: The size is irregular, and a small amount of new morphological structure (a needle-like morphology) appeared that can be assigned to ettringite [33]. However, a large number of rod-like structures also appeared

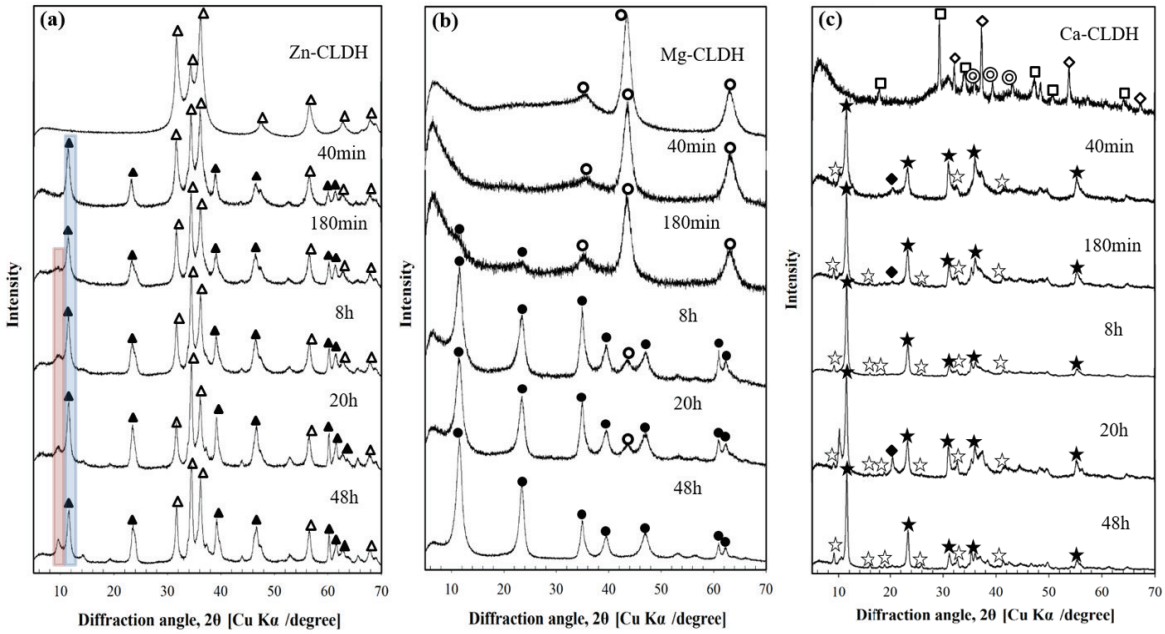

Fig. 3. XRD patterns of (a) Zn-CLDH, (b) Mg-CLDH, and (c) Ca-CLDH after sorption of 2.5 mM B under pH 7.0. Symbols: ▲, Zn-LDH; △, Zn-CLDH; ●, Mg-LDH; ○, Mg-CLDH; ★, Ca-LDH; □, $Ca(OH)_2$; ◇, CaO; ◎, $Ca_{12}Al_{14}O_{33}$; ☆, Borate-containing ettringite ($Ca_6[Al(OH)_6]_2[B(OH)_4]_6$); ◆, $CaCO_3$.

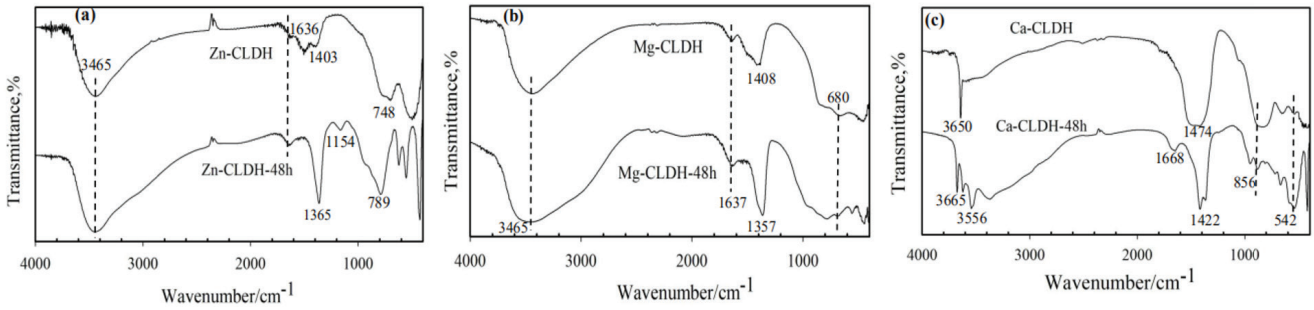

Fig. 4. FTIR patterns of (a) Zn-CLDH, (b) Mg-CLDH, and (c) Ca-CLDH before and after sorption 2.5 Mm B under pH 7.0.

in the SEM of Ca-CLDH (2:1) after the adsorption [22]. These changes in each type of CLDHs are consistent with the previous XRD results and further indicate that the mechanisms of boron species removal with Zn-CLDH, Mg-CLDH, and Ca-CLDH are also different.

Fig. S5(a) shows the survey XPS spectrum of Zn-CLDHs (3:1) after the adsorption of boron. This clearly shows that mainly Zn, Al, B, and C are present in the product. In Fig. S5(b), a peak at 191.47 can be assigned to B–O [34]. The electron binding energy peaks of aluminum (Fig. S5(c)) were well-identified at ~74 eV (Al 2p). The results show that Al exists as the oxide/hydroxide chemical states. The major peak has a binding energy of 1021.41eV (Fig. S5(d)), corresponding to the binding energy of Zn 2p3/2 [35]. Fig. S5(e) shows the high-resolution C1s XPS spectra. Two peaks of C=O and C–C/C–H appeared at 284.4 and 289.12 eV, respectively [36].

Fig. S6(a) shows the survey XPS spectrum of Mg-CLDHs (3:1) after the adsorption of boron. This clearly shows that mainly Mg, Al, B, and C are present in the product. As shown in Fig. S6(b), a peak appeared at 191.51 eV that can be assigned to the B–O bond [34]. The electron binding energy peaks of Al and Zn (Figs. S6(c) and S6(d)) are well-identified at ~74 eV (Al 2p) and 88 eV (Mg 2s), respectively. The results show that Al and Mg exist in the oxide/hydroxide chemical states [37]. Fig. S6(e) shows the high-resolution C1s XPS spectra. Two peaks of C=O and C–C/C–H appeared at 284.4 and 288.12 eV, respectively [36].

Fig. S7(a) shows the survey XPS spectrum of Ca-CLDHs (3:1) after the adsorption of boron. This clearly shows that mainly Ca, Al, B, and C are present in the product. As shown in Fig. S5(b), a peak appeared at 191.58 eV that can be clearly assigned to the B–O bond [34]. The electron binding energy peak of Al (Fig. S7(c)) is well-identified at ~74 eV (Al 2p). The results show that Al exists in the oxide/hydroxide chemical states. In Fig. S7(d), the peaks at 346.79 and 350.32 eV correspond to Ca 2p3/2 and Ca 2p1/2, respectively [38]. Fig. S7(e) shows the high-resolution C1s XPS spectra. Two peaks of C=O and C–C/C–H appeared at 284.4 and 289.12 eV, respectively [36].

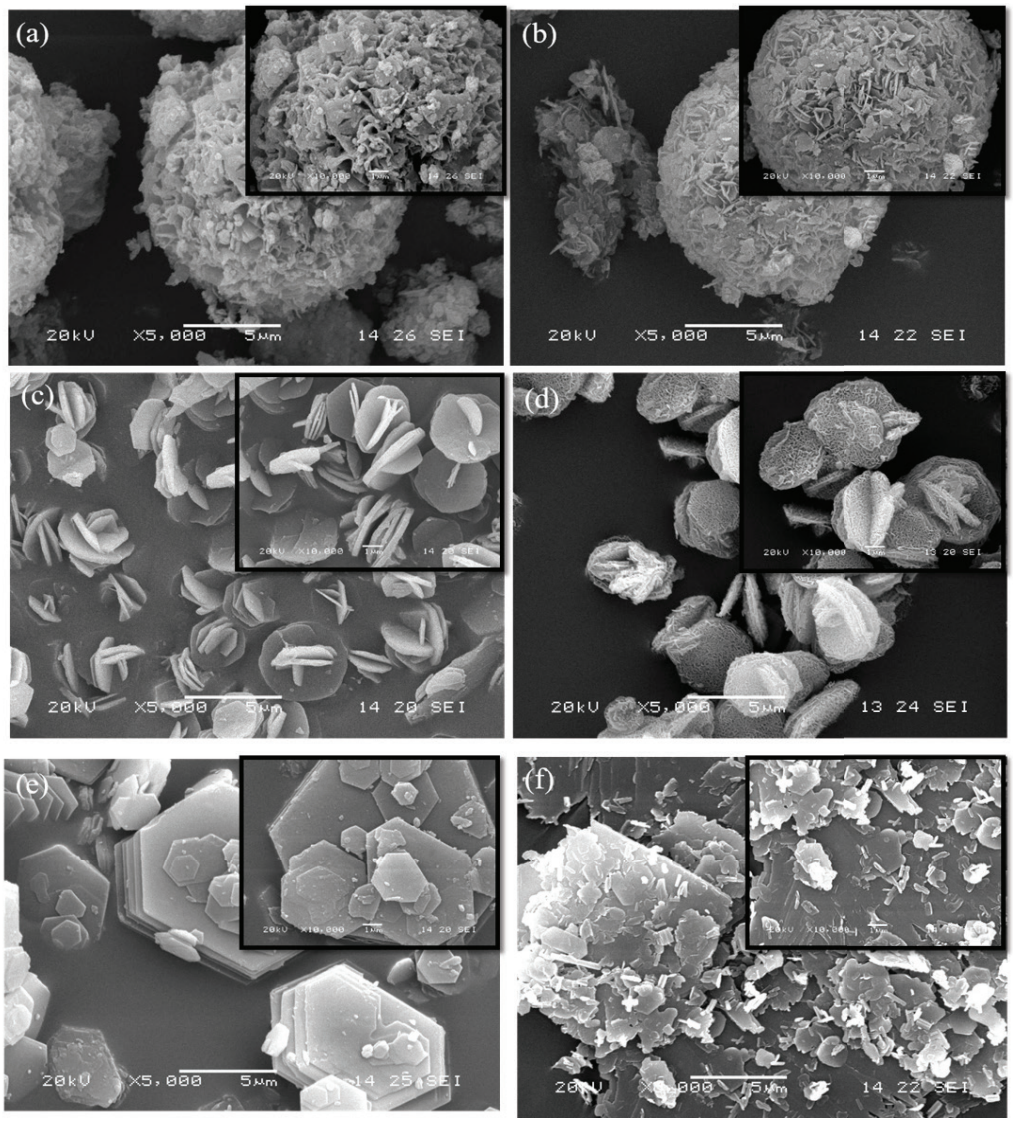

Fig. 5. SEM images of (a) Zn-LDH, (b) Zn-CLDH after sorption of B, (c) Mg-LDH, (d) Mg-CLDH after sorption of B, (e) Ca-LDH, and (f) Ca-CLDH after sorption of B. Insets show the expanded SEM images of particle surface with 1 μm of horizontal bars.

3.3. Discussion

3.3.1. Removal mechanism of borate with Zn-CLDH

First, when Zn-CLDH (3:1) (a special bimetallic oxide) is added to a 2.5 mmol/L borate solution, Zn^{2+} and Al^{3+} are eluted into the solution, but their concentrations are maintained at very low levels (as shown in Fig. 2), the same as Zn-CLDH (2:1) (as shown in Fig. S1) [22]. Because the initial pH of borate solution is 7 and the pKa of $Zn(OH)_2$ is 6.1, which is lower than that of $Mg(OH)_2$, under these conditions, Zn^{2+} is more likely to react with OH^- to form a hydroxide precursor than Mg^{2+} and can react with Al^{3+} more quickly to form ZnAl-LDH. The result of experiment is also the same (Fig. 3); this also applies to Zn(Mg)-Al-LDH (2:1)(Fig. S1) [22].

According to the small interlayer spacing of regenerated Zn-LDHs and the result of FTIR, within 40 min of reaction, it is known that the intercalated anion in Zn-LDHs is CO_3^{2-} or OH^-; the process are shown in Eqs. (1) and (2) [39].

$$Zn_3AlO_{4.5} + 4.5H_2O \rightleftarrows Zn_3Al(OH)_8 \cdot OH^- \quad (1)$$

$$Zn_3AlO_{4.5} + CO_3^{2-} + 4.5H_2O \rightleftarrows Zn_3Al(OH)_8 \cdot CO_3^{2-} + OH^- \quad (2)$$

In the meantime, Zn-CLDHs are also transformed into Zn-LDHs through boron species in the solution, as expressed by Eq. (3).

$$Zn_3AlO_{4.5} + B(OH)_4^- + 4.5H_2O \rightleftarrows Zn_3Al(OH)_6 \cdot B(OH)_4 + 3OH^- \quad (3)$$

However, the positive charge carried by its host layer requires a large amount of interlayer anions for neutralization. Therefore, during the regeneration, the boron species in

the solution are aggregated to cause polymerization, changing the interlayer anions. At this time, the pH of solution is ~9 (Fig. 2).The process is shown in Eqs. (4)–(6).

$$B(OH)_4^- \rightleftarrows B(OH)_3 + OH^- \quad (4)$$

$$2B(OH)_3 + 2B(OH)_4^- \rightleftarrows B_4O_5(OH)_4^{2-} + 5H_2O \quad (5)$$

$$4Zn_3Al(OH)_8 \cdot B(OH)_4 \rightleftarrows \left[Zn_3Al(OH)_8\right]_2 \cdot B_4O_5(OH)_4 + 2Zn_3Al(OH)_8 \cdot OH + 5H_2O \quad (6)$$

Because the ionic sizes of $B_4O_5(OH)_4^{2-}$ are larger than OH^- and $B(OH)_4^-$, Zn-LDH (3:1) with larger layer distances are formed after 8 h as shown in the XRD pattern (Fig. 3), and the corresponding diffraction peak intensity increases slowly as the reaction occurs. However, Zn-LDH (2:1) with a larger layer spacing was formed at 3 h, and its diffraction peak is strong [22]. However, this peak almost disappeared in the subsequent spectrum, because $B_4O_5(OH)_4^{2-}$ decomposed into $B(OH)_3$ and $B(OH)_4^-$ in the anionic layers of LDHs (as shown in Fig. S2).

In the meantime, the composite metal oxide continues to transform into Zn-LDHs as the reaction time increases; more LDHs can accommodate a large amount of boron species, further decreasing the borate concentration. However, it takes more than 8 h for the boric acid to be completely adsorbed by Zn-CLDH (3:1), while Zn-CLDH (2:1) only takes 3 h to achieve better results.

Through the above analysis, the following conjecture can be made. Because of the structure regeneration of Zn-CLDH (3:1), $B(OH)_4^-$ and $B(OH)_3$ enter the interlayer, but a large number of electrostatic adsorption sites gradually increases the size of interlayer ions, resulting in the partial polymerization of boric acid. The borates are gradually adsorbed in a polymer and free form. The adsorption site of regenerated Zn-LDH (2:1) is relatively scattered, because less metal ions are present on the laminate than Zn-LDH (3:1). Therefore, it takes some time to polymerize boric acid due to weak electrostatic adsorption force. Therefore, a large amount of boric acid polymerizes in a short time, so that the borate concentration rapidly decreases by Zn-CLDH (2:1) at 3 h of reaction.

Thus, when the ion ratio of metal laminate changes, Zn-CLDHs would show a difference in the adsorption of boric acid. This also indicates that the proportion of LDHs should be considered when boric acid is adsorbed by Zn-CLDH. The mechanism of borate removal with Zn-CLDHs is shown in Fig. 6.

3.3.2. Removal mechanism of borate with Mg-CLDH

At the beginning of reaction, the major boron species have two forms of $B(OH)_4^-$ and $B(OH)_3$ when the boron concentration is lower than 25 mmol/L [18]. Therefore, the following reaction occurs by electrostatic adsorption [Eq. (7)]

$$\equiv Mg(Al)OH_2^+ + B(OH)_4^- \rightarrow \equiv Mg(Al)OH_2^+ — B(OH)_4^- \quad (7)$$

In the meantime, $B(OH)_3$ mainly reacts with ≡Al–OH and ≡Mg–OH as follows [Eqs. (8) and (9)] [16].

$$\equiv Al - OH + B(OH)_3 \rightarrow \equiv Al — H_2BO_3 + H_2O \quad (8)$$

$$\equiv Mg - OH + B(OH)_3 \rightarrow \equiv Mg — H_2BO_3 + H_2O \quad (9)$$

Therefore, at initial pH 7 and when the borate concentration is 2.5 mmol/L, $B(OH)_4^-$, and $B(OH)_3$ are adsorbed on the oxide surface, which is the first step to remove borate. Mg-CLDHs dissolves Mg^{2+} and Al^{3+} and simultaneously produces OH^- at the beginning of reaction, as shown in Eqs. (10) and (11).

$$MgO + H_2O \rightarrow Mg^{2+} + 2OH^- \quad (10)$$

$$Al_2O_3 + H_2O \rightarrow 2Al^{3+} + 6OH^- \quad (11)$$

Therefore, the pH of solution will increase, and the metal ion concentration will also increase, but after Mg-CLDH (3:1) reaction for 8 h, the metal ion concentration is reduced to the lowest level and remains stable (Fig. 2). However, the metal ion concentration of Mg-CLDH (2:1) gradually decreases to a minimum until 48 h (Fig. S1) [22]. This is because the increase in pH causes the conversion of Mg^{2+} and Al^{3+} to hydroxides. Corresponding to the change in metal ion concentration, the pH of Mg-CLDH (3:1) increases to above 10 at 8 h, whereas the pH of Mg-CLDH (2:1) reached to 10 at 48 h [Eqs. (12) and (13)]

$$Mg^{2+} + 2OH^- \rightarrow Mg(OH)_2 \quad (12)$$

$$Al^{3+} + 4OH^- \rightarrow Al(OH)_4^- \quad (13)$$

Then, with increasing reaction time, the metal oxide is gradually dissolved, $Mg(OH)_2$ will react with boron species and $Al(OH)_4^-$ and transform into Mg-LDHs [Eq. (14)] [40].

$$x\,Mg(OH)_2 + Al(OH)_4^- + B(OH)_4^- \rightleftarrows Mg_xAl(OH)_{2+2x} \cdot B(OH)_4 + 2OH^- \quad (14)$$

This is the second step of boron species removal by Mg-CLDHs, because $B(OH)_4^-$ in solution was acquired to balance the charge. Therefore, after 8 h of reaction, the borate concentration hardly decreases with Mg-CLDH (3:1), and the Mg-LDH (3:1) is found in the XRD pattern at 8 h (Fig. 3). However, borate is completely adsorbed with Mg-CLDH (2:1) only after 48 h of reaction, and the regenerated Mg-LDH (2:1) appears in the XRD pattern only at the same time (Fig. S3) [22]. In addition, as previously reported [21], the formation of $Mg(OH)_2 \cdot H_3BO_3$ through the reaction between MgO and H_3BO_3 at this stage acts as a sink to attract the borate into the interlayer of Mg-LDH. This is because of the first step that the regeneration time of Mg-CLDHs becomes longer, mainly because of the presence of Mg^{2+} in the metal oxide. Because of

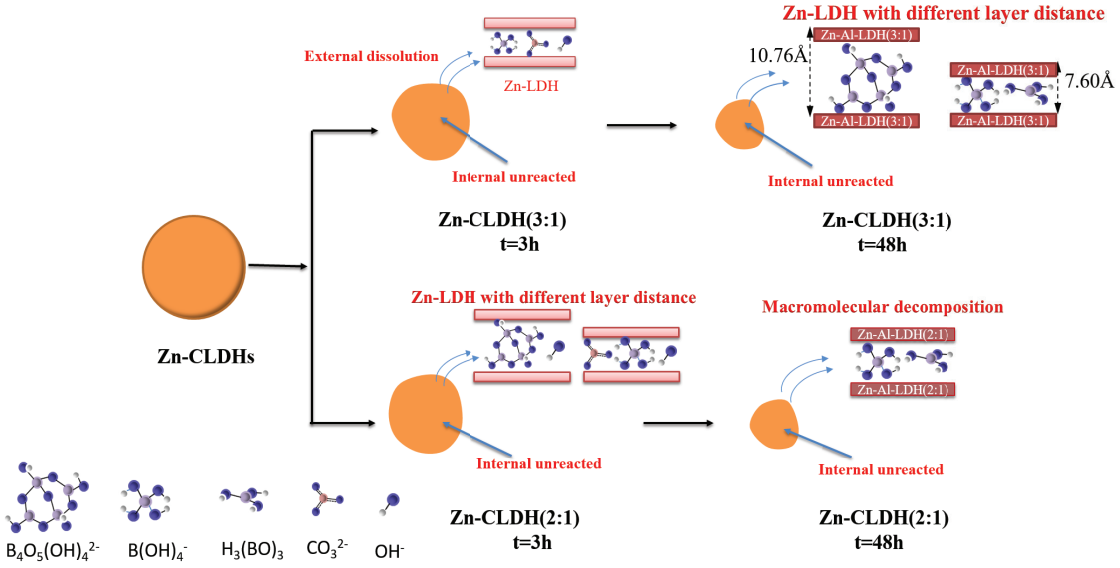

Fig. 6. Schematic illustration of sorption mechanism of borate onto Zn-CLDHs.

its special chemical properties, it causes a series of chemical reactions with the solution, resulting in the removal mechanism of boric acid different from other CLDHs.

In the meantime, because the regeneration of Mg-CLDHs is a mixture of dissolution and reprecipitation, the regenerated LDH forms small pieces on a large hexagonal plate, as shown in Fig. 5.

Based on the above analysis, the following conjecture can be made. One of the mechanisms of borate removal with Mg-CLDHs is electrostatic adsorption. Moreover, the amount of metal cations of Mg-CLDH (3:1) is more, resulting in more adsorption sites. Therefore, a large amount of borate is adsorbed on the surface of Mg-CLDH (3:1). At the same time, the pH increases faster in the solution, so that the Mg-LDH (3:1) can be regenerated more quickly. However, because of a fewer adsorption sites and slow increase in pH, Mg-CLDH (2:1)in Mg-LDH (2:1) was regenerated until 48 h. These results show that when the ratio of bivalent metal ions to trivalent metal ions in LDH changes, it has a certain influence on the adsorption of boric acid. The sorption mechanism of borate removal with Mg-CLDHs is shown in Fig. 7.

3.3.3. Borate removal mechanism with Ca-CLDH

When Ca-CLDHs are added to a borate solution, the metal oxide reacts to release Ca^{2+}, Al^{3+}, and OH^-, increasing the metal ion concentration and pH of the solution (as shown in Figs. 2 and S1). As the reaction continues, Al^{3+} becomes $Al(OH)_4^-$ in an alkaline environment and then reacts with $Ca(OH)_2$ to form CaAl-LDHs. Because the affinity of OH^- and CO_3^{2-} with the host layer in Ca-LDH is stronger than that of $B(OH)_4^-$, the sorption sites are more easily occupied by OH^- and CO_3^{2-}.

$$Ca_6Al_2O_5(OH)_8 + 5H_2O \rightleftarrows 2Ca_3Al(OH)_8 \cdot OH \quad (15)$$

$$Ca_6Al_2O_5(OH)_8 + 5H_2O + CO_3^{2-} \rightleftarrows [Ca_3Al(OH)_8]_2 \cdot CO_3 + 2OH^- \quad (16)$$

However, Ca-LDH is more unstable than other LDHs, because the electronic structure of divalent cation is different, influencing the relative stability of corresponding cluster. The period number of Ca^{2+} is greater than that of Zn^{2+} and Mg^{3+}, which is negatively correlated with the binding energies of clusters [41]. It is in an equilibrium of dissolution–precipitation, resulting in a constant presence of Mg^{2+} and Al^{3+} in the solution as the following process [42,43].

$$Ca_3Al(OH)_8 \cdot OH \rightleftarrows 3Ca^{2+} + Al(OH)_4^- + 5OH^- \quad (17)$$

$$[Ca_3Al(OH)_8]_2 \cdot CO_3 \rightleftarrows 6Ca^{2+} + 2Al(OH)_4^- + 8OH^- + CO_3^{2-} \quad (18)$$

Then, the dissolved species react with $B(OH)_4^-$ to form borate-containing ettringite ($Ca_6[Al(OH)_6]_2[B(OH)_4]_6$), because borate is more likely to form ettringite than other oxyanions [44,45].

$$6Ca^{2+} + 2Al(OH)_4^- + 6B(OH)_4^- + 4OH^- \rightleftarrows Ca_6[Al(OH)_6]_2[B(OH)_4]_6 \quad (19)$$

Therefore, the boron concentration decreased (Figs. 2 and S1), as observed from the characteristic diffraction peaks of ettringite at 40 min of XRD pattern (Figs. 3 and S3). However, with the increase in reaction time, the boron concentration of Ca-CLDH (3:1) remained stable after 3 h, and the intensity of characteristic peaks of ettringite did not increase as shown in the XRD pattern. This is different with Ca-CLDH (2:1), because the XRD pattern (Fig. S4) shows that the peaks of borate-containing ettringite gradually increases, and the main peak of Ca-LDH (2:1) gradually decreases [22]. Thus, by comparison, under the same experimental conditions, Ca-CLDH (2:1) is more suitable for the formation of ettringite

with the increase in reaction time, whereas because of the characteristics of its own structure, Ca-CLDH (3:1) hinders the formation of ettringite, resulting in poor adsorption.

Moreover, although the characteristic diffraction peaks of $CaCO_3$ are observed in the XRD pattern of Ca-CLDH (3:1), it is negligible (Fig. 3). However, in the XRD pattern of Ca-CLDH (2:1), the peaks of $CaCO_3$ are obvious (Fig. S3) [22]. The formation of $CaCO_3$ is due to the released Ca^{2+} from Ca-LDH and reaction of ettringite with CO_3^{2-} in the solution. [46] It has been reported that $CaCO_3$ may react with boron, decreasing the borate concentration.

Based on the above results, the following conjecture can be made. The formation of ettringite is influenced by the environment of solution, especially pH [47]. However, the solution pH during the sorption of Ca-CLDH (3:1) and Ca-CLDH (2:1) is almost the same, but it can be found that the dissolution of metal ions in the solution is very different between them (Figs. 2 and S1). The concentration of Ca^{2+} and Al^{3+} in the solution of Ca-CLDH (2:1) is much higher than that of Ca-CLDH (3:1), probably the reason why Ca-CLDH (2:1) can form ettringite during the reaction. The mechanism of borate removal with Ca-CLDHs is shown in Fig. 8.

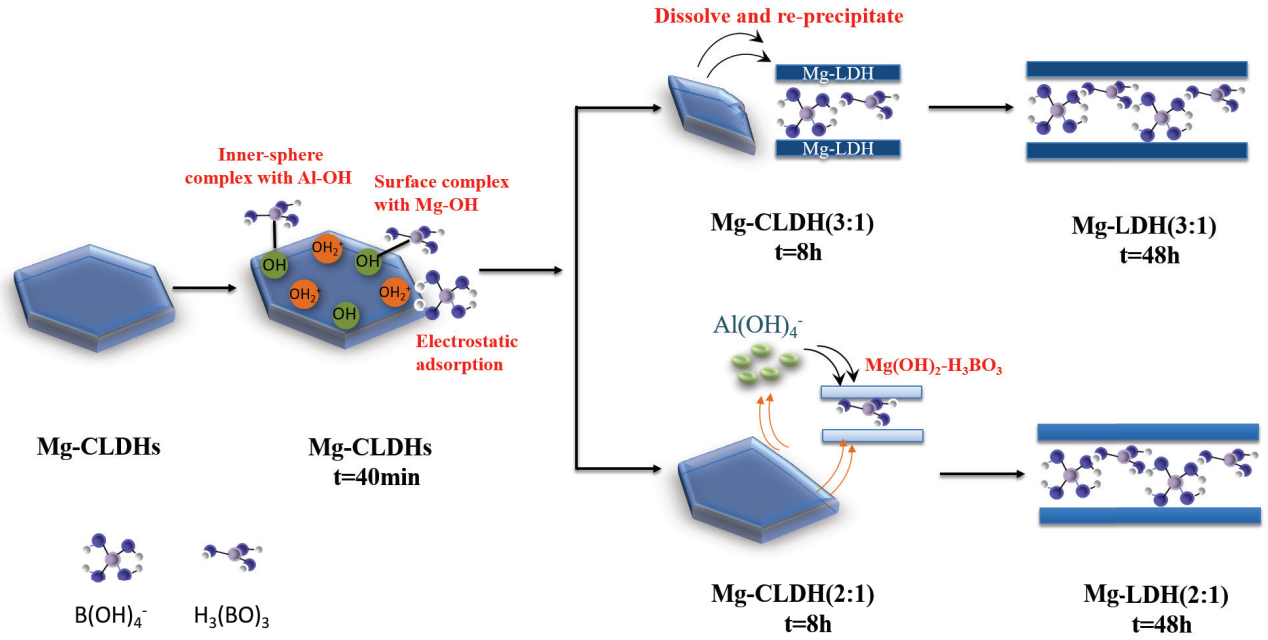

Fig. 7. Schematic illustration of sorption mechanism of borate onto Mg-CLDHs.

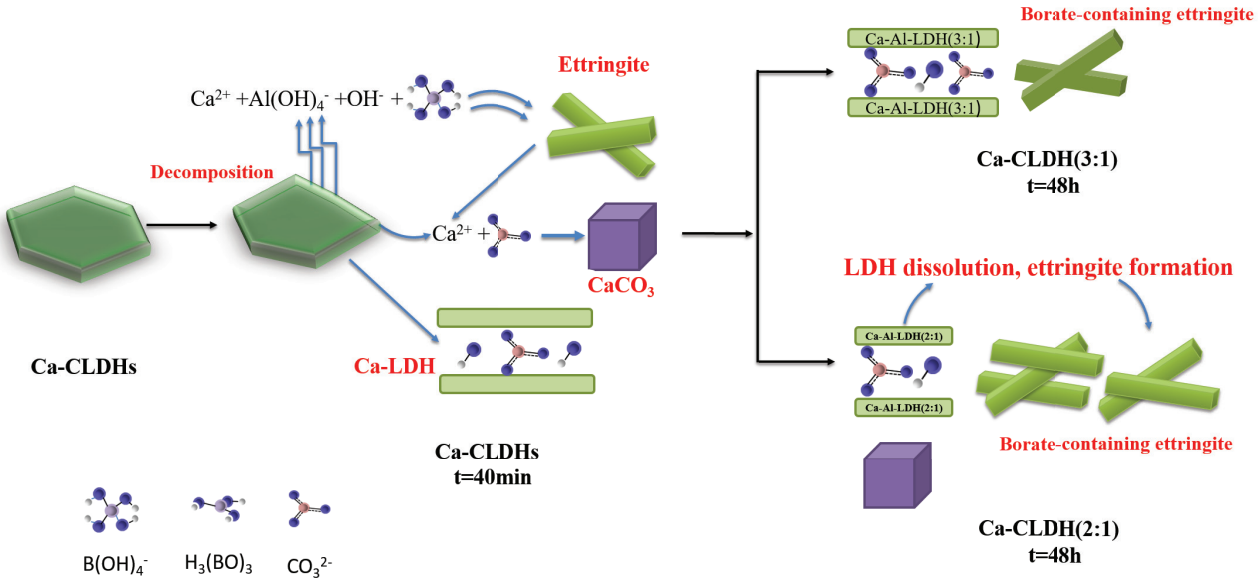

Fig. 8. Schematic illustration of sorption mechanism of borate onto Ca-CLDHs.

4. Conclusions

Based on the above analysis, CLDHs containing different divalent metal ions have different mechanisms for borate removal. This is because different CLDHs containing different divalent metal ions differ in their crystal structure, crystal morphology, alkalinity, and electronegativity of anions. At the same time, because of different ratios of divalent and trivalent ions in the metal laminate, the CLDHs (2:1 and 3:1) produce different adsorption results in the treatment of boric acid.

By comprehensively considering the XRD, FTIR, and SEM analyses, it was observed that the main mechanism of borate adsorption by Zn-CLDHs is through anion exchange and intercalation. Although the final sorption effect is similar, Zn-LDH (2:1) containing polymerized boron formed at 3 h and almost disappeared afterwards. However, Zn-LDH (3:1) began to form after 3 h and gradually increased. For Mg-CLDHs, the borate concentration is reduced by surface adsorption reaction and intercalation. Moreover, the group formed on the surface of Mg-CLDHs fixes the boron species. This is an important reason why the borate concentration decreases. Because the regeneration time of Mg-CLDH (3:1) was only 8 h, whereas Mg-CLDH (2:1) needed 48 h, Mg-CLDH (3:1) had a better effect than Mg-CLDH (2:1). In particular, Ca-CLDHs converted to Ca-LDHs immediately, but Ca-LDHs are very easy to dissolve due to structural characteristics. Therefore, the borate-containing ettringite is formed through the ions dissolved from the Ca-LDHs and borate in the solution. This is the main borate removal mechanism of Ca-CLDHs. However, the amount of ettringite produced by Ca-CLDH (3:1) during the adsorption is constant, resulting in poor adsorption. On the other hand, Ca-CLDH (2:1) could continue to generate ettringite during the reaction, thus gradually decreasing the borate concentration.

Acknowledgments

This work was supported by the National Natural Science Foundation of China (51504170 and 51374157), Nature Science Foundation of Hubei Province of China (2015CFB166), and Graduate Education Innovation Foundation of Wuhan Institute of Technology (CX2018157).

References

[1] F.J. Murray, A human health risk assessment of boron (boric acid and borax) in drinking water, Regul. Toxicol. Pharmacol., 22 (1995) 221–230.
[2] R.J.Weir Jr, R.S. Fisher, Toxicologic studies on borax and boric acid, Toxicol. Appl. Pharm., 23 (1972) 351–364.
[3] A. Waggott, An investigation of the potential problem of increasing boron concentrations in rivers and water courses, Water Res., 3 (1969) 749–765.
[4] B. Bertagnolli, A. Grishin, T. Vincent, E. Guibal, Boron removal by a composite sorbent: Polyethylenimine/tannic acid derivative immobilized in alginate hydrogel beads, J. Environ. Sci. Health Part A Toxic/Hazard Subst. Environ. Eng., 52 (2016) 359–367.
[5] N. Hilal, G.J. Kim, C. Somerfield, Boron removal from saline water: a comprehensive review, Desalination, 273 (2011) 23–35.
[6] X. Qiu, K. Sasaki, T. Hirajima, K. Ideta, M. Jin, Temperature effect on the sorption of borate by a layered double hydroxide prepared using dolomite as a magnesium source, Chem. Eng. J., 225 (2013) 664–672.
[7] Z. Gao, S. Xie, B. Zhang, X. Qiu, F. Chen, Ultrathin Mg-Al layered double hydroxide prepared by ionothermal synthesis in a deep eutectic solvent for highly effective boron removal, Chem. Eng. J., 15 (2017) 89–97.
[8] M.R. Pastor, A.F. Ruiz, M.F. Chillón, D.P. Rico, Influence of pH in the elimination of boron by means of reverse osmosis, Desalination,140 (2001) 145–152.
[9] H. Hyung, J.H. Kim, A mechanistic study on boron rejection by sea water reverse osmosis membranes, J. Membr. Sci., 286 (2006) 269–278.
[10] H. Liu, B. Qing, X. Ye, L. Quan, K. Lee, Z. Wu, Boron adsorption by composite magnetic particles, Chem. Eng. J.,151 (2009) 235–240.
[11] O.P. Ferreira, S.G. de Moraes, N. Durán, L. Cornejo, O.L. Alves, Evaluation of boron removal from water by hydrotalcite-like compounds, Chemosphere, 62 (2006) 80–88.
[12] R. Kunin, A.F. Preuss, Characterization of a boron-specific ion exchange resin, Ind. Eng. Chem. Prod. Res. Dev., 3 (1964) 304–306.
[13] M.M. Nasef, M. Nallappan, Z. Ujang, Polymer-based chelating adsorbents for the selective removal of boron from water and wastewater: a review, React. Funct. Polym., 85 (2014) 54–68.
[14] H. Zhou, Z. Wen, J. Liu, J. Ke, X. Duan, S. Wang, Z-scheme plasmonic Ag decorated WO_3/Bi_2WO_6 hybrids for enhanced photocatalytic abatement of chlorinated-VOCs under solar light irradiation, Appl. Catal. B., 242 (2019) 76–84.
[15] J. Ke, M.A. Younis, Y. Kong, H. Zhou, J. Liu, L. Lei, Y. Hou, Nanostructured ternary metal tungstate-based photocatalysts for environmental purification and solar water splitting: a review, Nano-Micro Lett., 10 (2018) 69.
[16] Y.H. Teow, A.W. Mohammad, New generation nanomaterials for water desalination: a review, Desalination, 451 (2019) 2–17.
[17] L. Kentjono, J.C. Liu, W.C. Chang, C. Irawan, Removal of boron and iodine from optoelectronic wastewater using Mg-Al (NO_3) layered double hydroxide, Desalination, 262 (2010) 280–283.
[18] F.L. Theiss, G.A. Ayoko, R.L. Frost, Removal of boron species by layered double hydroxides: a review, J. Colloid Interface Sci., 402 (2013) 114–121.
[19] E.D. Isaacs-Paez, R. Leyva-Ramos, A. Jacobo-Azuara, J.M. Martinez-Rosales, J.V. Flores-Cano, Adsorption of boron on calcined Al-Mg-layered double hydroxide from aqueous solutions. Mechanism and effect of operating conditions, Chem. Eng. J., 245 (2014) 248–257.
[20] A. Demetriou, I. Pashalidis, A.V. Nicolaides, M.U. Kumke, Surface mechanism of the boron adsorption on alumina in aqueous solutions, Desalin. Wat. Treat., 51 (2013) 6130–6136.
[21] K. Sasaki, X. Qiu, S. Moriyama, C. Tokoro, J. Miyawaki, J. Miyawaki, Characteristic sorption of $H_3BO_3/B(OH)_4^-$ on magnesium oxide, Mater. Trans., 54 (2013) 3837–3844.
[22] X. Qiu, K. Sasaki, K. Osseo-Asare, T. Hirajima, K. Ideta, J. Miyawaki, Sorption of $H_3BO_3/B(OH)_4^-$ on calcined LDHs including different divalent metals, J. Colloid Interface Sci., 445 (2015) 183–194.
[23] H. Yan, M. Wei, J. Ma, D.G. Evans, X. Duan, Plane-wave density functional theory study on the structural and energetic properties of cation-disordered Mg−Al layered double hydroxides, J. Phys. Chem. A., 114 (2010) 7369–7376.
[24] H. Yan, M. Wei, J. Ma, X. Duan, Density functional theory study on the influence of cation ratio on the host layer structure of Zn/Al double hydroxides, Particuology, 8 (2010) 212–220.
[25] Z. Gao, K.Sasaki, X. Qiu, Structural memory effect of Mg−Al and Zn−Al layered double hydroxides in the presence of different natural humic acids: process and mechanism, Langmuir, 34 (2018) 5386−5395.
[26] F. Millange, R.I. Walton, D. O'Hare, Time-resolved in situ X-ray diffraction study of the liquid-phase reconstruction of Mg-Al-carbonate hydrotalcite-like compounds, J. Mater. Chem., 10 (2000) 1713–1720.
[27] Y. Xu, Y. Dai, J. Zhou, Z.P. Xu, G. Qian, G.Q.M. Lu, Removal efficiency of arsenate and phosphate from aqueous solution using layered double hydroxide materials: intercalation vs. precipitation, J. Mater. Chem., 20 (2010) 4684–4691.

[28] J.P. Jolivet, M. Henry, J. Livage, Metal Oxide Chemistry and Synthesis: from Solution to Solid State, John Wiley & Sons, vol. 46, pp. 21–30, 2000.
[29] Y. Hiraga, N. Shigemoto, Removal of as and se oxoanions from solution using calcination products of $Ca(OH)_2$-$Al(OH)_3$ and $CaCO_3$-$Al(OH)_3$ mixtures, J. Chem. Eng. Jpn., 45 (2012) 554–562.
[30] T. Lv, W. Ma, G. Xin, R. Wang, J. Xu, D. Liu, F. Liu, D. Pan, Physicochemical characterization and sorption behavior of Mg-Ca-Al (NO_3) hydrotalcite-like compounds toward removal of fluoride from protein solutions, J. Hazard. Mater., 237–238 (2012) 121–132.
[31] K. Abdellaoui, I. Pavlovic, M. Bouhent, A. Benhamou, C. Barriga, A comparative study of the amaranth azo dye adsorption/desorption from aqueous solutions by layered double hydroxides, Appl. Clay Sci., 143 (2017) 142–150.
[32] P. Koilraj, S. Kannan, Phosphate uptake behavior of ZnAlZr ternary layered double hydroxides through surface precipitation, J. Colloid Interface Sci., 341 (2010) 289–297.
[33] T. Hongo, Y. Tsunashima, Y. Sakai, A. Iizuka, A. Yamasaki, A comparative borate adsorption study of Ettringite and Metaettringite, Chem. Lett., 40 (2011) 1269–1271.
[34] B.J. Feng, J. Zhang, Q. Zhong, W.B. Li, S. Li, H. Li, P. Cheng, S. Meng, L. Chen, K.H. Wu, Experimental realization of two-dimensional boron sheets, Nat. Chem., 8 (2016) 563–568.
[35] J. Sun, Y. Zhang, J. Cheng, H. Fan, J. Zhu, X. Wang, S. Ai, Synthesis of Ag/AgCl/Zn-Cr LDHs composite with enhanced visible-light photocatalytic performance, J. Mol. Catal. A: Chem., 382 (2014) 146–153.
[36] S. Reiche, R. Blume, X.C. Zhao, D. Su, E. Kunkes, M. Behrens, R. Schlögl, Reactivity of mesoporous carbon against water—an in-situ XPS study, Carbon, 77 (2014) 175–183.
[37] N. Chubar, V. Gerda, O. Megantari, M. Mičušík, M. Omastova, K. Heister, P. Man, J. Fraissard, Applications versus properties of Mg–Al layered double hydroxides provided by their syntheses methods: alkoxide and alkoxide-free sol–gel syntheses and hydrothermal precipitation, Chem. Eng. J., 234 (2013) 284–299.
[38] L.-J. Wang, J.-P. Yu, K.-C. Chou, S. Seetharaman, Effects of MgO and Al_2O_3 addition on redox state of chromium in CaO-SiO_2-CrOx slag system by XPS method, Metall. Mater. Trans. B., 46 (2015) 1802–1808.
[39] Z.M. Ni, S.J. Xia, L.G. Wang, F.F. Xing, G.X. Pan, Treatment of methyl orange by calcined layered double hydroxides in aqueous solution: adsorption property and kinetic studies, J. Colloid Interface Sci., 316 (2007) 284–291.
[40] Z.P. Xu, G.Q. Lu, Hydrothermal synthesis of layered double hydroxides (LDHs) from mixed MgO and Al_2O_3: LDH formation mechanism, Chem. Mater., 17 (2005) 1055–1062.
[41] H. Yan, M. Wei, J. Ma, F. Li, D.G. Evans, X. Duan, Theoretical study on the structural properties and relative stability of M(II)-Al layered double hydroxides based on a cluster model., J. Phys. Chem. A., 113 (2009) 6133–6141.
[42] J.W. Boclair, P.S. Braterman, Layered double hydroxide stability. 1. Relative stabilities of layered double hydroxides and their simple counterparts, Chem. Mater., 11 (1999) 298–302.
[43] G. Qian, L. Feng, J.Z. Zhou, Y. Xu, J. Liu, J. Zhang, Z.P. Xu, Solubility product (Ksp)-controlled removal of chromate and phosphate by hydrocalumite, Chem. Eng. J., 181–182 (2012) 251–258.
[44] Y. Hiraga, N. Shigemoto, Boron uptake behavior during ettringite synthesis in the presence of H_3BO_3 and in a suspension of ettringite in H_3BO_3, J. Chem. Eng. Jpn., 43 (2010) 865–871.
[45] M. Chrysochoou, D. Dermatas, Evaluation of ettringite and hydrocalumite formation for heavy metal immobilization: literature review and experimental study, J. Hazard. Mater., 136 (2006) 551–560.
[46] N.G. Hemming, G.N. Hanson, Boron isotopic composition and concentration in modern marine carbonates, Geochim. Cosmochim. Acta, 56 (1992) 537–543.
[47] A.M. Cody, H. Lee, R.D. Cody, P.G. Spry, The effects of chemical environment on the nucleation, growth, and stability of ettringite $[Ca_3Al(OH)_6]_2(SO_4)_3 \bullet 26H_2O$, Cem. Concr. Res., 34 (2004) 869–881.
[48] L.V. Rajaković, M.D. Ristić, Sorption of boric acid and borax by activated carbon impregnated with various compounds, Carbon, 34 (1996) 769–774.
[49] S. Karahan, M. Yurdakoç, Y. Seki, K. Yurdakoç, Removal of boron from aqueous solution by clays and modified clays, J. Colloid Interface Sci., 293 (2006) 36–42.
[50] Y. Cengeloglu, A. Tor, G. Arslan, M. Ersoz, S. Gezgin, Removal of boron from aqueous solution by using neutralized red mud, J. Hazard. Mater., 142 (2007) 412–417.
[51] U. Mezuman, R. Keren, Boron adsorption by soils using a phenomenological adsorption equation, Soil Sci. Soc. Am. J., 45 (1981) 722–726.
[52] K. Sasaki, X.H. Qiu, Y. Hosomomi, S. Moriyama, T. Hirajima, Effect of natural dolomite calcination temperature on sorption of borate onto calcined products, Microporous Mesoporous Mater., 171 (2013) 1–8.
[53] T. Qi, A. Sonoda, Y. Makita, H. Kanoh, K. Ooi, T. Hirotsu T, Synthesis and borate uptake of two novel chelating resins, Ind. Eng. Chem. Res., 41 (2002) 133–138.
[54] A. Harada, T. Takagi, S. Kataoka, T. Yamamoto, A. Endo, Boron adsorption mechanism on polyvinyl alcohol, Adsorption, 17 (2017) 171–178.
[55] X.H. Qiu, K. Sasaki, T. Hirajima, K. Ideta, J. Miyawaki, Temperature effect on the sorption of borate by a layered double hydroxide prepared using dolomite as a magnesium source, Chem. Eng. J., 225 (2013) 664–672.
[56] P. Koilraj, K. Srinivasan, High sorptive removal of borate from aqueous solution using calcined ZnAl layered double hydroxides, Ind. Eng. Chem. Res., 50 (2011) 6943–6951.
[57] X.H. Qiu, K. Sasaki, K. Osseo-Asare, T. Hirajima, K. Ideta, J. Miyawaki, Sorption of $H_3BO_3/B(OH)_4^-$ on calcined LDHs including different divalent metals, J. Colloid Interface Sci., 445 (2015) 183–194.

Supplementary material

Table S1

Adsorbent	Adsorption capacity (mmol/g)	References
Activated carbon	3.7×10^{-2}	[48]
Bentonite	1.3×10^{-2}	[49]
Red mud	8.9×10^{-1}	[50]
Illite	1.5×10^{-3}	[51]
Kaolinite	2.9×10^{-3}	[51]
Calcined dolomite	1.5	[52]
IRA 743 (Commercial resin)	0.91	[53]
CRB 05 (Commercial resin)	1.3	[54]
Mg-Al-LDH (2:1)	0.9	[55]
Calcined Mg-Al-LDH	2.37	[55]
Zn-Al-LDH (2:1)	1.3	[56]
Calcined Zn-Al-LDH	2.9	[56]

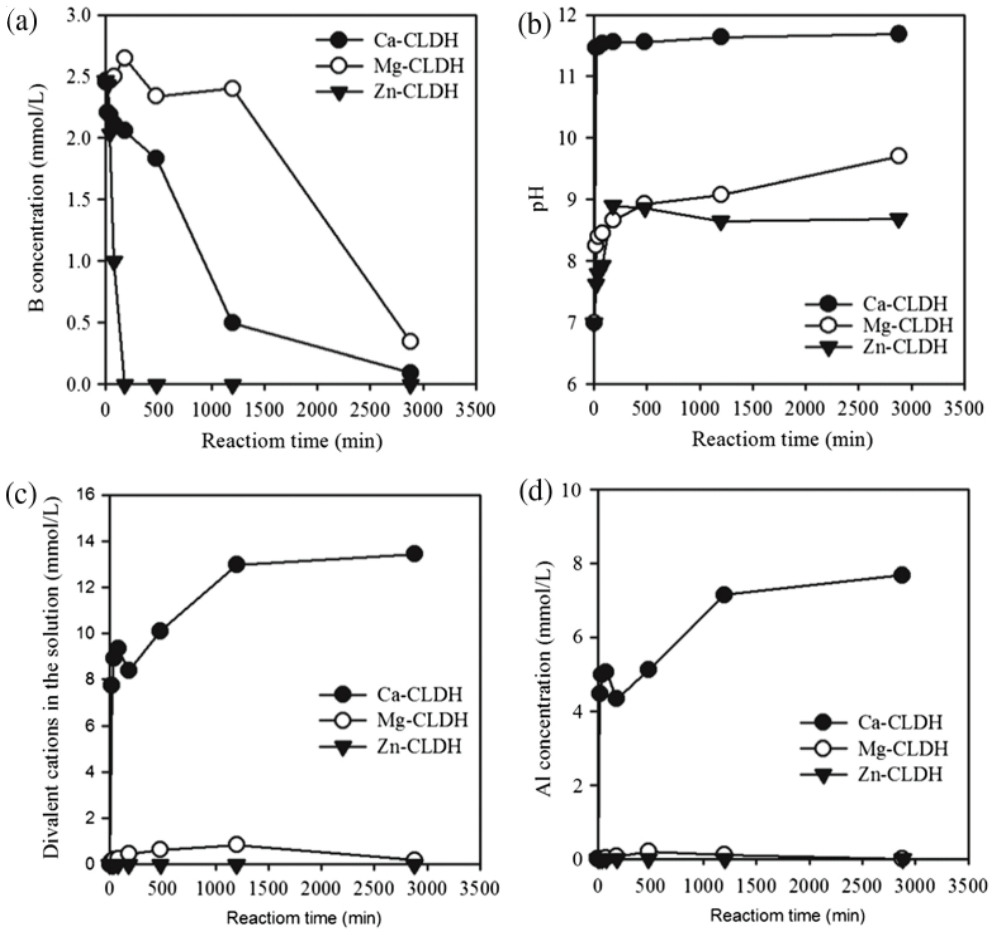

Fig. S1. Changes of (a) B concentrations, (b) pH, (c) divalent cations concentration and (d) Al concentration during sorption of 2.5mM B by MgAl-CLDH, ZnAl-CLDH, and CaAl-CLDH. Amount of sorbent: 2.5 g/L; initial B concentration: 2.5mM; initial pH: 7.0. (M^{2+}:M^{3+} = 2:1) [57].

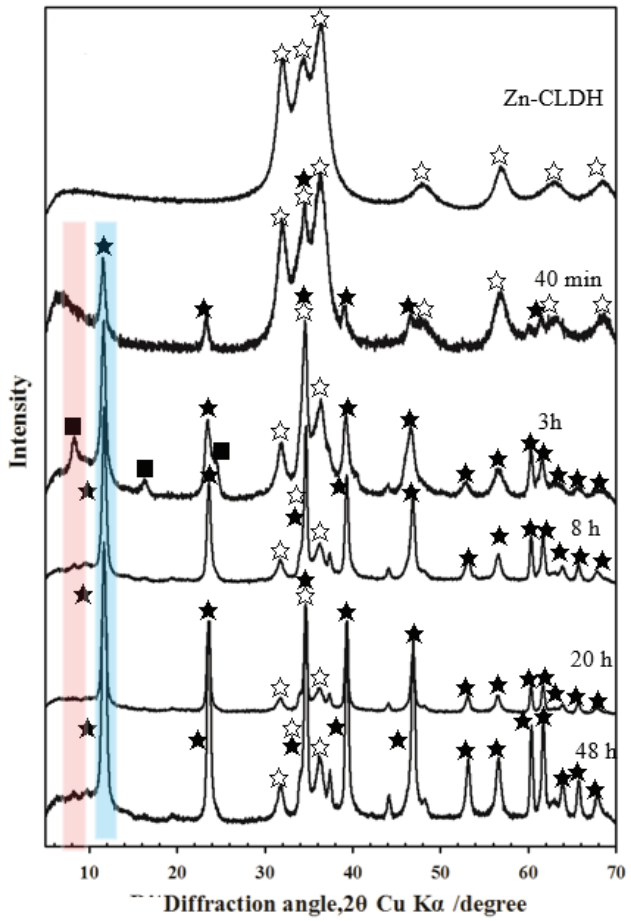

Fig. S2. XRD patterns of ZnAl-CLDH (Zn^{2+}:Al^{3+} = 2:1) after sorption of 2.5mM B. under pH 7.0. Symbols: ★, Zn-LDH; ☆, Zn-CLDH; ■, Zn-LDH with larger interlayer distance [57].

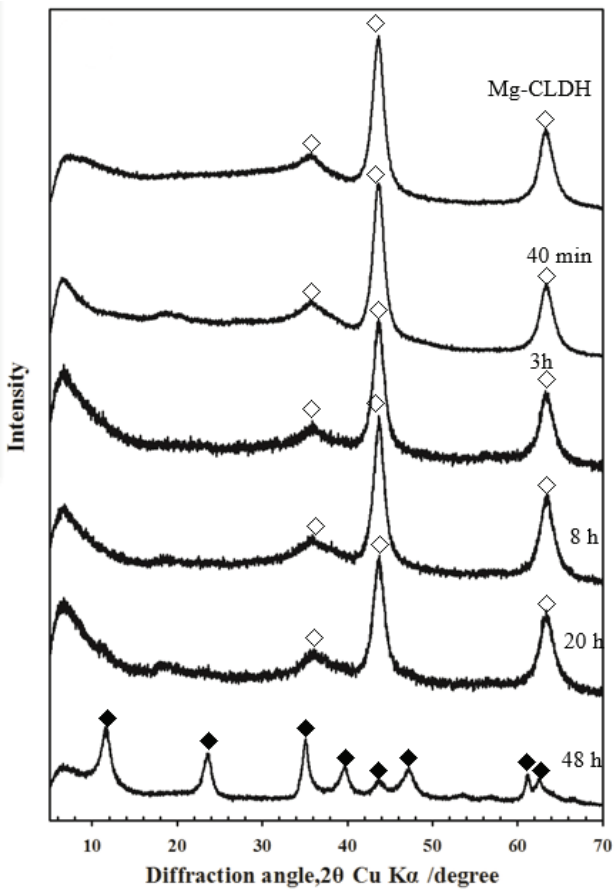

Fig. S3. XRD patterns of MgAl-CLDH (Mg^{2+}:Al^{3+} = 2:1) after sorption of 2.5mM B. under pH 7.0. Symbols: ◆, Mg-LDH; ◇, Mg-CLDH [57].

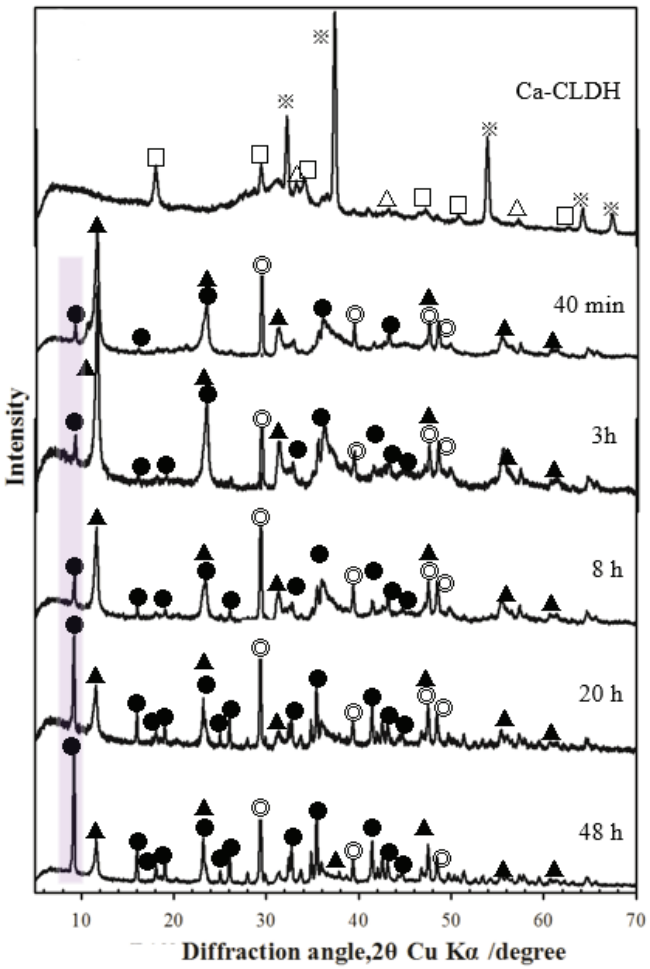

Fig. S4. XRD patterns of CaAl-CLDH (Ca^{2+}:Al^{3+} = 2:1) after sorption of 2.5mM B. under pH 7.0. Symbols: ▲, Ca-LDH; □, $Ca(OH)_2$; ※ CaO; △, $Ca_{12}Al_{14}O_{33}$; ●, Borate-containing ettringite ($Ca_6[Al(OH)_6]_2[B(OH)_4]_6$); ◎, $CaCO_3$ [57].

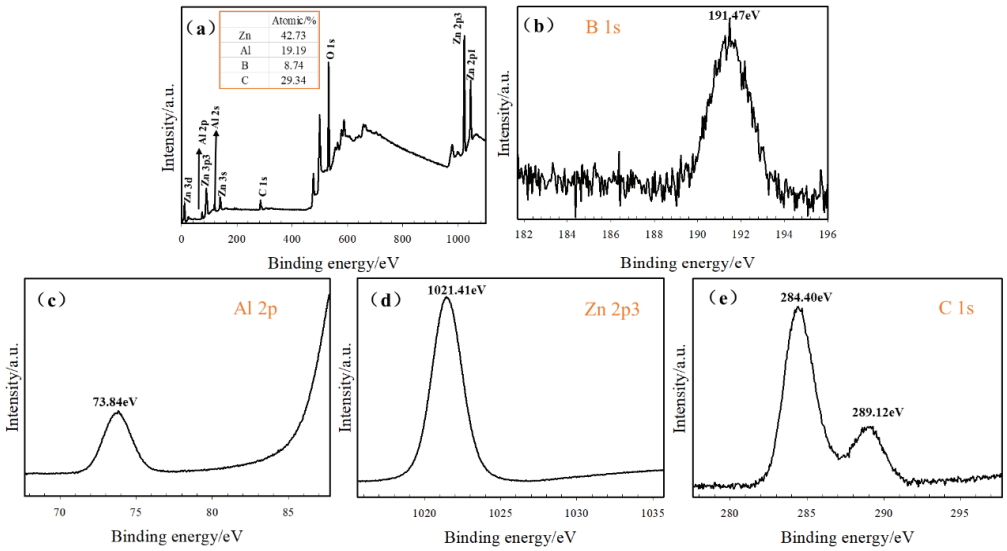

Fig. S5. The XPS full spectrum and individual elemental spectra of Zn-CLDH (3:1) after adsorption of 2.5 mM B (T = 48 h). (a) Full-scale survey, (b) B 1s spectrum, (c) Al 2p spectrum, (d) Zn 2p3 spectrum, (e) C 1s spectrum.

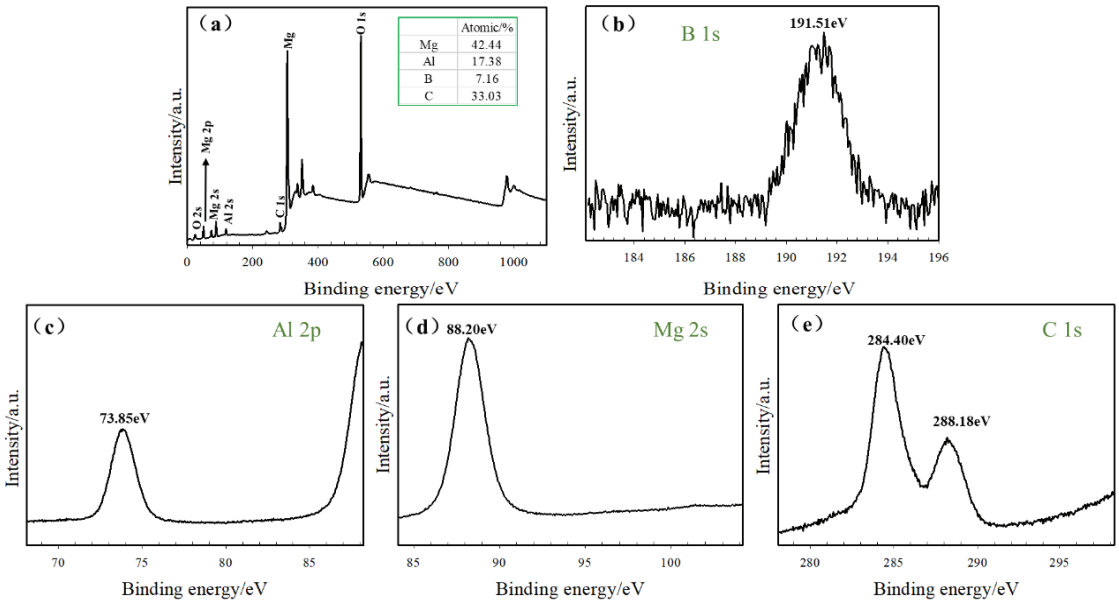

Fig. S6. The XPS full spectrum and individual elemental spectra of Mg-CLDH (3:1) after adsorption of 2.5 mM B (T = 48 h). (a) Full-scale survey, (b) B 1s spectrum, (c) Al 2p spectrum, (d) Mg 2sspectrum, (e) C 1s spectrum.

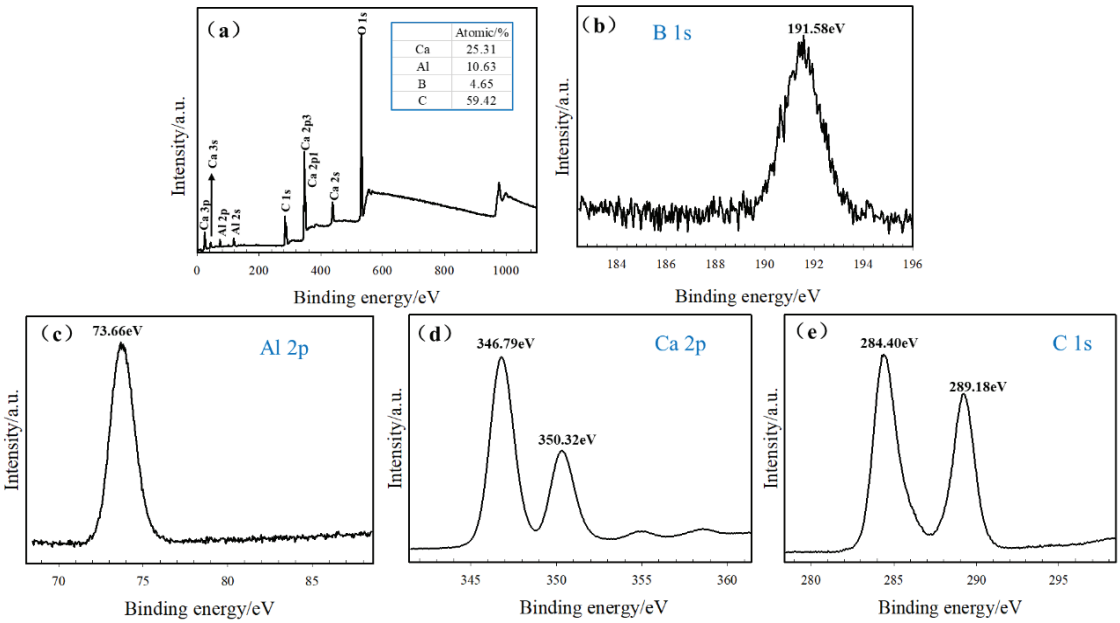

Fig. S7. The XPS full spectrum and individual elemental spectra of Ca-CLDH (3:1) after adsorption of 2.5 mM B (T = 48 h). (a) Full-scale survey, (b) B 1s spectrum, (c) Al 2p spectrum, (d) Ca 2p spectrum, (e) C 1s spectrum.